

Thermal Conductivity and Magnetic Phase Diagram of CuB_2O_4

Takayuki Kawamata¹, Naoki Sugawara¹, Siyed Mohammad Haidar¹, Tadashi Adachi², Takashi Noji¹, Kazutaka Kudo³, Norio Kobayashi⁴, Yutaka Fujii⁵, Hikomitsu Kikuchi⁶, Meiro Chiba⁶, German A. Petrakovskii⁷, Mikhail A. Popov⁷, Leonard N. Bezmaternykh⁷, and Yoji Koike¹

¹*Department of Applied Physics, Tohoku University, Sendai 980-8579, Japan*

²*Department of Engineering and Applied Sciences, Sophia University, Tokyo 102-8554, Japan*

³*Research Institute for Interdisciplinary Science, Okayama University, Okayama 700-8530, Japan*

⁴*Institute for Materials Research, Tohoku University, Sendai 980-8577, Japan*

⁵*Research Center for Development of Far-Infrared Region, University of Fukui, Fukui 910-8507, Japan*

⁶*Department of Applied Physics, Faculty of Engineering, University of Fukui, Fukui 910-8507, Japan*

⁷*Institute of Physics, Siberian Branch of the Russian Academy of Science, 660036 Krasnoyarsk, Russia*

(Received)

We have measured temperature and magnetic field dependences of the thermal conductivity along the c -axis, κ_c , and that along the [110] direction, κ_{110} , of CuB_2O_4 single crystals in zero field and magnetic fields along the c -axis and along the [110] direction. It has been found that the thermal conductivity is nearly isotropic and very large in zero field and that the thermal conductivity due to phonons is dominant in CuB_2O_4 . The temperature and field dependences of κ_c and κ_{110} have markedly changed at phase boundaries in the magnetic phase diagram, which has been understood to be due to the change of the mean free path of phonons caused by the change of the phonon-spin scattering rate at the phase boundaries. It has been concluded that thermal conductivity measurements are very effective for detecting magnetic phase boundaries.

1. Introduction

In insulating quantum spin systems, the thermal conductivity is expressed as the sum of the thermal conductivity due to spins, namely, due to magnetic excitations, κ_{spin} , and the thermal conductivity due to phonons, κ_{phonon} , and is sensitive to the change of the spin state such as magnetic phase transitions. It is of course that κ_{spin} changes in accordance with the change of the spin state. Moreover, κ_{phonon} also changes in accordance with the change of the spin state owing to the resultant change of the phonon-spin scattering rate, $1/\tau_{\text{phonon-spin}}$, where $\tau_{\text{phonon-spin}}$ is the relaxation time of the scattering between phonons and magnetic excitations. Therefore, the thermal conductivity measurement is a good probe to investigate the change of the spin state. In fact, an increase in κ_{phonon} has been observed in the spin gap state of CuGeO_3 ,^{1,2)} $\text{SrCu}_2(\text{BO}_3)_2$,³⁻⁶⁾ TlCuCl_3 ,⁷⁾ and in the magnetization-plateau state of $\text{Cu}_3(\text{CO}_3)_2(\text{OH})_2$.⁸⁾ In several antiferromagnetic materials, moreover, an increase in the thermal conductivity has been observed just below the antiferromagnetic transition temperature.⁹⁻¹¹⁾

The compound CuB_2O_4 is a quantum spin system possessing two Cu sites, namely, Cu_A and Cu_B sites in the crystal structure, where Cu_A^{2+} ions with the spin quantum number $S = 1/2$ form a three-dimensional network of spins and Cu_B^{2+} ions with $S = 1/2$ form zigzag chains of spins along the c -axis, as shown in Fig. 1. Cu_A^{2+} and Cu_B^{2+} ions form Cu_AO_4 and Cu_BO_4 squares, respectively, which are connected with each other through a BO_4 tetrahedron. The magnitude of the interaction between Cu_A^{2+} spins has been estimated from the inelastic neutron-scattering experiment as 45 K.¹²⁾ Neither the interaction between Cu_B^{2+} spins nor the interaction between Cu_A^{2+} and Cu_B^{2+} spins has yet been clarified, but they are inferred to be weak.

The magnetic properties in CuB_2O_4 have been revealed by various studies.¹²⁻²⁸⁾ That is, CuB_2O_4 undergoes a transition from a paramagnetic phase (P phase) to a commensurate weak ferromagnetic one (C phase) of Cu_A^{2+} spins (Fig. 2(a)) at the transition temperature $T_N = 21$ K and a successive transition to an incommensurate helical one (IC phase) of Cu_A^{2+} and Cu_B^{2+} spins (Fig. 2(b)) at the transition temperature $T^* \sim 10$ K with decreasing temperature. It has been suggested that a magnetic soliton lattice is formed along the c -axis around T^* .¹⁶⁾ In fact, the elastic neutron-scattering experiment has confirmed the existence of an IC phase

related to the magnetic soliton lattice in magnetic fields of 1.0 - 1.5 T along the [110] direction in a narrow temperature-region below 4 K.²⁴⁾ By the application of magnetic fields parallel to the *ab*-plane and the *c*-axis, various magnetic phases have been reported to appear. The magnetic phase diagram is different between magnetic fields parallel to the *ab*-plane and the *c*-axis, while the anisotropy of the magnetic phase diagram within the *ab*-plane is very small.¹⁹⁾

The spin structure of CuB₂O₄ in zero field has also been revealed by the elastic neutron-scattering experiments.^{18,20)} In the C phase, as shown in Fig. 2(a), Cu_A²⁺ spins are almost pointing to the [110] direction and arranged ferromagnetically along the *c*-axis, while they are arranged antiferromagnetically in the *ab*-plane. The weak ferromagnetism is induced by the ~3° cant of Cu_A²⁺ spins within the *ab*-plane.^{18,20)} The Cu_B²⁺ spins are nearly paramagnetic with the small magnetic moment of 0.2 μ_B.²⁰⁾ In the IC phase, as shown in Fig. 2(b), both Cu_A²⁺ and Cu_B²⁺ spins are incommensurate along the *c*-axis and the wave number of the spin modulation continuously increases with decreasing temperature from $\mathbf{k} = (0, 0, 0)$ at T^* to $\mathbf{k} = (0, 0, 0.15)$ at $T = 1.8$ K.²⁰⁾ This is inferred to be due to the weak interaction between Cu_A²⁺ and Cu_B²⁺ spins.

Since the arrangement of spins is different between in the *ab*-plane and along the *c*-axis, in this paper, we have measured temperature and magnetic field dependences of the thermal conductivity along the *c*-axis, κ_c , and that along the [110] direction, κ_{110} , of CuB₂O₄ single crystals and investigated the spin state and magnetic phase diagram dependent on temperature and magnetic field. Here, we have selected the [110] direction in the *ab*-plane, because single crystals with long sizes along the [110] direction were obtained.

2. Experimental

Single crystals of CuB₂O₄ were grown by the flux method using CuO, B₂O₃, and Li₂CO₃ as flux.²⁹⁾ Thermal conductivity measurements of the single crystals with the size of 1×1×5 mm³ were carried out by the conventional four-terminal steady-state method, using two Cernox thermometers (LakeShore Cryotronics, Inc., CX-1050-SD). Magnetic fields were applied to the single crystals using a superconducting magnet.

3. Results and discussion

3.1 Thermal conductivity in zero field

Figure 3 shows the temperature dependences of κ_c and κ_{110} in zero field. It is found that both κ_c and κ_{110} are similar to each other and comparatively large among various compounds regarded as quantum spin systems. The both exhibit a peak at 40 K and are markedly enhanced just below T_N . Since CuB_2O_4 is a magnetic insulator where the thermal conductivity is given by the sum of κ_{phonon} and κ_{spin} , the enhancement just below T_N is understood to be due to the enhancement of κ_{spin} and/or κ_{phonon} . κ_{spin} increases owing to the increase in the mean free path of magnetic excitations, l_{spin} , on account of the increase in the magnetic correlation length in the long-range magnetically ordered state. On the other hand, κ_{phonon} increases owing to the increase in the mean free path of phonons, l_{phonon} , on account of the decrease in $1/\tau_{\text{phonon-spin}}$ in the ordered state. In the case of CuB_2O_4 , the enhancements of κ_c and κ_{110} just below T_N are as large as ~ 100 W/Km. This magnitude of the enhancement is comparable with values of κ_{spin} observed in low-dimensional quantum spin systems with the superexchange interaction between Cu^{2+} spins as large as ~ 2000 K such as $\text{Sr}_{14}\text{Cu}_{24}\text{O}_{41}$,³⁰⁻³⁵⁾ Sr_2CuO_3 ,³⁶⁻³⁹⁾ and SrCuO_2 .^{37,40,41)} The magnitude of κ_{spin} tends to increase with the increase in the interaction between spins. Taking into account the weaker interaction of 45 K between Cu_A^{2+} spins in CuB_2O_4 ¹²⁾ than the superexchange interaction in $\text{Sr}_{14}\text{Cu}_{24}\text{O}_{41}$, Sr_2CuO_3 , and SrCuO_2 , it is rather hard for the enhancements of κ_c and κ_{110} just below T_N to be regarded as being due to the enhancements of κ_{spin} . In this compound, therefore, it is concluded that κ_{phonon} is dominant and that the enhancements of κ_c and κ_{110} just below T_N are due to the enhancement of κ_{phonon} .

The inset of Fig. 3 shows enlarged plots of κ_c and κ_{110} at low temperatures to see the change around T^* in detail. It is found that the temperature dependence of κ_{110} exhibits a bend at T^* , namely, a marked decrease just below T^* , while that of κ_c does not. Since the magnetic specific heat, C_{spin} , has been reported to increase at T^* in CuB_2O_4 ,¹³⁾ κ_{spin} , which is given by the product of C_{spin} , the velocity of magnetic excitations, v_{spin} , and l_{spin} , should increase just below T^* , but actually κ_{110} decreases just below T^* . Therefore, the bend at T^* is regarded as being due to the decrease in κ_{phonon} just below T^* . Since κ_{phonon} is given by the product of the specific heat of phonons, C_{phonon} , the velocity of phonons, v_{phonon} , and l_{phonon} ,

the decrease in κ_{phonon} means the decrease in either of them just below T^* . If C_{phonon} decreased just below T^* , the bend should be observed not only in κ_{110} but also in κ_c . In general, the change of v_{phonon} is too small to induce such a large change of κ_{110} at T^* , because the dispersion of phonons little changes without any structural phase transition. Accordingly, the decrease in κ_{110} just below T^* is regarded as being due to the decrease in l_{phonon} , namely, the decrease in $1/\tau_{\text{phonon-spin}}$ along the [110] direction. No bent in κ_c at T^* indicates that l_{phonon} along the c -axis direction does not markedly change. The decrease in l_{phonon} along the [110] direction just below T^* is inferred to be due to the shortening of the magnetic correlation length along the [110] direction. In fact, the muon spin relaxation experiment has revealed that the muon spin relaxation rate decreases below T^* .^{18,22)} This means that the Cu^{2+} spins are fluctuating fast beyond the μSR time window. Therefore, this is reasonably interpreted as being due to the enhancement of spin fluctuations caused by the shortening of the magnetic correlation length along the [110] direction below T^* .

Here, we discuss the origin of the shortening of the magnetic correlation length only along the [110] direction below T^* . In the C phase at temperatures between T^* and T_N , Cu_A^{2+} spins are arranged ferromagnetically along the c -axis, while they are arranged antiferromagnetically in the ab -plane. Cu_B^{2+} spins are still nearly paramagnetic and the interaction between Cu_B^{2+} spins is negligible. Considering a triangle formed by two adjacent Cu_A^{2+} spins along the c -axis and their nearest neighboring Cu_B^{2+} spin, as shown in Fig. 2(a), there is no frustration between the Cu_A^{2+} and Cu_B^{2+} spins, because Cu_A^{2+} spins are ferromagnetic along the c -axis. Considering a triangle formed by two adjacent Cu_A^{2+} spins along the a -axis (b -axis) and their nearest neighboring Cu_B^{2+} spin, as shown in Fig. 2(a), on the other hand, there is frustration between the Cu_A^{2+} and Cu_B^{2+} spins, because Cu_A^{2+} spins are antiferromagnetic in the ab -plane. Accordingly, when Cu_B^{2+} spins get to be ordered below T^* , the magnetic correlation length in the ab -plane is understood to become shorter than that along the c -axis owing to the frustration, leading to the decrease in only κ_{110} just below T^* .

3.2 Thermal conductivity in magnetic fields

Figures 4(a) and 4(b) display the temperature dependences of κ_{110} in magnetic fields

along the [110] direction and along the c -axis, respectively. Every temperature dependence of κ_{110} exhibits a marked enhancement just below T_N . Therefore, the marked enhancement is regarded as being due to the enhancement of κ_{phonon} in magnetic fields as well as in zero field. Figures 4(c) and 4(d) show the temperature dependences of κ_{110} divided by T^3 , κ_{110}/T^3 , in magnetic fields along the [110] direction and along the c -axis, respectively, to see the change around T^* in detail by suppressing the influence of C_{phonon} proportional to T^3 at low temperatures. In magnetic fields, there are anomalies similar to that observed at T^* in zero field. It is found that T^* decreases with increasing field. In magnetic field of 0.9 T parallel to the [110] direction, moreover, κ_{110}/T^3 shows a sudden enhancement at ~ 5.4 K with decreasing temperatures, as shown by an arrow in Fig. 4(c).

Figures 5(a) and 5(b) display magnetic phase diagrams in magnetic fields parallel to the ab -plane and along the c -axis, respectively, obtained from the ESR,^{14,19,27)} neutron scattering,²⁴⁾ nonlinear optical,²¹⁾ NMR,^{25,26)} μSR ,²²⁾ and magnetization²⁸⁾ measurements. In the phase diagram in magnetic fields along the ab -plane, here, we call the IC phase at lower fields and at higher fields IC(I) and IC(II), respectively. In the IC(II) phase, the elastic neutron-scattering experiment has revealed that commensurate and small incommensurate modulations coexist.²⁴⁾ In the IC(I) phase, spin-flop transitions have been observed in nonlinear optical²¹⁾ and magnetization²⁸⁾ measurements. Here, we call the IC(I) phase at higher and lower temperatures than the spin-flop transition temperature IC(I)-H and IC(I)-L, respectively.

The temperatures where κ_{110} changes markedly, shown by arrows in Figs. 4(a) - 4(d), are plotted by closed circles in Figs. 5(a) and 5(b). It is found that T_N and T^* obtained from κ_{110} is in correspondence with the phase boundary detected by the nonlinear optical,²¹⁾ neutron scattering,²⁴⁾ and magnetization²⁸⁾ measurements. The observed point at ~ 5.4 K in a magnetic field of 0.9 T is also in correspondence with the phase boundary of the spin-flop transition between IC(I)-H and IC(I)-L phases.

Figures 6(a) and 6(b) display the magnetic field dependences of κ_{110} at low temperatures in magnetic fields along the [110] direction and along the c -axis, respectively. At 5.5 K, the magnetic field dependence is anisotropic depending on the field direction and no hysteresis is observed. It is found that κ_{110} changes markedly at several magnetic fields, as

shown by arrows in Figs. 6(a) and 6(b). The magnetic fields where κ_{110} changes markedly, shown by arrows in Figs. 6(a) and 6(b), are plotted by open circles in Figs. 5(a) and 5(b).

In Fig. 6(a), the marked change of κ_{110} at 1.6 T in magnetic fields along the [110] direction at 5.5 K is in good correspondence with the phase boundary between C and IC(II) phases detected by the neutron scattering²⁴⁾ and NMR²⁵⁾ measurements. The decrease in κ_{110} below 1.6 T is reasonably understood to be due to the transition to the IC(II) phase. Furthermore, two kinks at ~ 0.7 T and ~ 1.1 T in κ_{110} are in correspondence with the phase boundaries between the IC(II), IC(I)-H, and IC(I)-L phases. In magnetic fields along the [110] direction at 3.2 K, κ_{110} shows a rapid decrease at ~ 1.4 T with increasing field. The magnetic field of ~ 1.4 T is in good correspondence with the phase boundary between the IC(I) and IC(II) phases via the narrow region of the soliton lattice phase detected by the inelastic neutron-scattering experiment.²⁴⁾

The difference of the magnetic correlation length between the IC(II), IC(I)-H, and IC(I)-L phases can be investigated from the magnetic field dependence of the magnitude of κ_{110} , because C_{phonon} and v_{phonon} is usually independent of magnetic field and only l_{phonon} is dependent on magnetic field. It is found from the field-dependence of κ_{110} at 5.5 K that the sudden drop at ~ 0.7 T with increasing field is due to the longer magnetic correlation length in the IC(I)-L phase than in the IC(I)-H one. Although the difference of the spin structure between the IC(I)-L and IC(I)-H phases has not been known, this result suggests that the frustration in the *ab*-plane may be released by the spin-flop phase transition from the IC(I)-H phase to IC(I)-L one. In the IC(II) phase, the magnitude of κ_{110} gradually increases with increasing field so as to connect the IC(I)-H phase to the C phase, indicating that the magnetic correlation length in the IC(II) phase also increases gradually with increasing field. Since commensurate and small incommensurate modulations coexist in the IC(II) phase,²⁴⁾ the ratio of the commensurate region to the incommensurate region may increase with increasing field.

As for the magnetic field dependence of κ_{110} in magnetic fields along the *c*-axis at 5.5 K shown in Fig. 6(b), κ_{110} is found to start to increase from ~ 3 T with increasing field, which may be related to the phase boundary due to the ferroelectric phase transition suggested by the ESR experiment.²³⁾ It is noted that no change has been observed in the temperature dependences of κ_{110} shown in Figs. 4(b) nor 4(d) at the phase boundary due to the

ferroelectric phase transition, while some change has been observed in the magnetic field dependence of κ_{110} shown in Fig. 6(b). This is understood as follows. That is, not only l_{phonon} but also C_{phonon} is temperature-dependent at low temperatures, while C_{phonon} is usually independent of magnetic field so that only l_{phonon} is magnetic field-dependent. In order to detect only the change of l_{phonon} , therefore, measurements of the magnetic field dependence of κ_{110} are more sensitive than those of the temperature dependence of κ_{110} .

After all, it has been found that the points, where κ_{110} changes markedly, are approximately on the phase boundaries obtained by various measurements.¹³⁻²⁸⁾ Therefore, it is concluded that thermal conductivity measurements are very effective for detecting magnetic phase boundaries in CuB_2O_4 also.

4. Summary

We have measured the temperature and magnetic field dependences of κ_c and κ_{110} of CuB_2O_4 single crystals. It has been found that both κ_c and κ_{110} are similar to each other and comparatively large and that the both exhibit a peak at 40 K and are markedly enhanced just below T_N in zero field. It has been concluded that κ_{phonon} is dominant in CuB_2O_4 and that the enhancements of κ_c and κ_{110} just below T_N are due to the increase in l_{phonon} caused by the formation of the commensurate weak ferromagnetic phase of Cu_A^{2+} spins. Moreover, it has been found that only κ_{110} exhibits a marked decrease just below T^* , which has been regarded as being due to the decrease in l_{phonon} owing to the decrease in the magnetic correlation length along the [110] direction caused by the frustration between Cu_A^{2+} and Cu_B^{2+} spins in the ab -plane of the IC phase. In magnetic fields along the [110] direction and along the c -axis, a marked enhancement of κ_{110} just below T_N has been observed as well as in zero field. The anomaly of κ_{110} observed at T^* in zero field has been observed in magnetic fields also. It has been found that T^* decreases with increasing field. The magnetic field dependences of κ_{110} at low temperatures in magnetic fields along the [110] direction and along the c -axis have revealed that they are anisotropic depending on the field direction and that κ_{110} changes markedly at several magnetic fields. The points, where κ_{110} changes markedly, have been found to be in correspondence with the phase boundaries obtained by various measurements.¹³⁻²⁸⁾ Accordingly, it has been concluded that thermal conductivity

measurements are very effective for detecting magnetic phase boundaries.

Acknowledgments

The thermal conductivity measurements in magnetic fields were performed at the High Field Laboratory for Superconducting Materials, Institute for Materials Research, Tohoku University. This work was supported by a Grant-in-Aid for Scientific Research of the Ministry of Education, Culture Sports, Science and Technology, Japan, (Grant Number: 17038002) and also by CREST of Japan Science and Technology Corporation. Figures 1 and 2 were drawn using VESTA.⁴²⁾

References

- 1) Y. Ando, J. Takeya, D. L. Sisson, S. G. Doettinger, I. Tanaka, R. S. Feigelson, and A. Kapitulnik, *Phys. Rev. B* **58**, R2913 (1998).
- 2) B. Salce, L. Devoille, R. Calemczuk, A. I. Buzdin, G. Dhalenne, and A. Revcolevschi, *Phys. Lett. A* **245**, 127 (1998).
- 3) K. Kudo, T. Noji, Y. Koike, T. Nishizaki, and N. Kobayashi, *J. Phys. Soc. Jpn.* **70**, 1448 (2001).
- 4) M. Hofmann, T. Lorenz, G. S. Uhrig, H. Kierspel, O. Zabara, A. Freimuth, H. Kageyama, and Y. Ueda, *Phys. Rev. Lett.* **87**, 047202 (2001).
- 5) A. N. Vasil'ev, M. M. Markina, A. V. Inyushkin, and H. Kageyama, *JETP Lett.* **73**, 933 (2001).
- 6) K. Kudo, T. Noji, Y. Koike, T. Nishizaki, and N. Kobayashi, *J. Phys. Soc. Jpn.* **73**, 3497 (2004).
- 7) K. Kudo, M. Yamazaki, T. Kawamata, T. Noji, Y. Koike, T. Nishizaki, N. Kobayashi, and H. Tanaka, *J. Phys. Soc. Jpn.* **73**, 2358 (2004).
- 8) Y. Hagiya, T. Kawamata, K. Naruse, M. Ohno, Y. Matsuoka, H. Sudo, H. Nagasawa, H. Kikuchi, T. Sasaki, and Y. Koike, *J. Phys. Soc. Jpn.* **85**, 034715 (2016).
- 9) G. A. Slack and R. Newman, *Phys. Rev. Lett.* **1**, 359 (1958).
- 10) G. A. Slack, *Phys. Rev.* **122**, 1451 (1961).
- 11) F. B. Lewis and N. H. Saunders, *J. Phys. C: Solid State Phys.* **6**, 2525 (1973).
- 12) M. Boehm, S. Martynov, B. Roessli, G. A. Petrakovskii, and J. Kulda, *J. Magn. Magn. Mater.* **250**, 313 (2002).
- 13) G. A. Petrakovskii, D. Velikanov, A. Vorotinov, A. Balaev, K. Sablina, A. Amato, B. Roessli, J. Schefer, and U. Staub, *J. Magn. Magn. Mater.* **205**, 105 (1999).
- 14) A. I. Pankrats, G. A. Petrakovskii, and N. V. Volkov, *Phys. Solid State* **42**, 96 (2000).
- 15) G. A. Petrakovskii, M. A. Popov, B. Roessli, and B. Ouladdiaf, *J. Exp. Theor. Phys.* **93**, 926 (2001).
- 16) B. Roessli, J. Schefer, G. A. Petrakovskii, B. Ouladdiaf, M. Boehm, U. Staub, A. Vorotinov, and L. Bezmaternikh, *Phys. Rev. Lett.* **86**, 1885 (2001).
- 17) J. Schefer, M. Boehm, B. Roessli, G. A. Petrakovskii, B. Ouladdiaf, and U. Staub, *Appl.*

Phys. A **74**, S1740 (2002).

18) M. Boehm, B. Roessli, J. Schefer, B. Ouladdiaf, A. Amato, C. Baines, U. Staub, and G. A. Petrakovskii, *Physica B* **318**, 277 (2002).

19) A. I. Pankrats, G. A. Petrakovskii, M. A. Popov, K. A. Sablina, L. A. Prozorova, S. S. Sosin, G. Szimczak, R. Szimczak, and M. Baran, *JETP Lett.* **78**, 569 (2003).

20) M. Boehm, B. Roessli, J. Schefer, A. S. Wills, B. Ouladdiaf, E. Lelièvre-Berna, U. Staub, and G. A. Petrakovskii, *Phys. Rev. B* **68**, 024405 (2003).

21) R. V. Pisarev, I. Sanger, G. A. Petrakovskii, and M. Fiebig, *Phys. Rev. Lett.* **93**, 037204 (2004).

22) A. Fukaya, I. Watanabe, K. Yamada, and K. Nagamine, *J. Phys. Soc. Jpn.* **75**, 113705 (2006).

23) T. Fujita, Y. Fujimoto, S. Mitsudo, T. Idehara, K. Inoue, J. Kishine, Y. Kousaka, S. Yano, J. Akimitsu, and M. Motokawa, *J. Phys.: Conf. Ser.* **51**, 111 (2006).

24) Y. Kousaka, S. Yano, M. Nishi, K. Hirota, and J. Akimitsu, *J. Phys. Chem. Solid* **68**, 2170 (2007).

25) Y. Yasuda, H. Nakamura, Y. Fujii, H. Kikuchi, M. Chiba, Y. Yamamoto, H. Hori, G. Petrakovskii, M. Popov and L. Bezmaternikh, *J. Phys.: Condens. Matter* **19**, 145277 (2007).

26) Y. Yasuda, H. Nakamura, Y. Fujii, H. Kikuchi, M. Chiba, Y. Yamamoto, H. Hori, G. Petrakovskii, M. Popov and L. Bezmaternikh, *J. Magn. Magn. Mater.* **310**, 1392 (2007).

27) T. Fujita, Y. Fujimoto, S. Mitsudo, T. Idehara, T. Saito, Y. Kousaka, S. Yano, J. Akimitsu, J. Kishine, K. Inoue, and M. Motokawa, *J. Phys. Soc. Jpn.* **77**, 053702 (2008).

28) A. E. Petrova and A. I. Pankrats, *JETP* **126**, 506 (2018).

29) G. A. Petrakovskii, K. A. Sablina, D. A. Velikanov, A. M. Vorotynov, N. V. Volkov, and A. F. Bovina, *Crystallogr. Rep.* **45**, 853 (2000).

30) K. Kudo, S. Ishikawa, T. Noji, T. Adachi, Y. Koike, K. Maki, S. Tsuji, and K. Kumagai, *J. Low Temp. Phys.* **117**, 1689 (1999).

31) A.V. Sologubenko, K. Gianno, H. R. Ott, U. Ammerahl, and A. Revcolevschi, *Phys. Rev. Lett.* **84**, 2714 (2000).

32) C. Hess, C. Baumann, U. Ammerahl, B. Buchner, F. Heidrich-Meisner, W. Brenig, and A. Revcolevschi, *Phys. Rev. B* **64**, 184305 (2001).

- 33) K. Kudo, S. Ishikawa, T. Noji, T. Adachi, Y. Koike, K. Maki, S. Tsuji, and K. Kumagai, J. Phys. Soc. Jpn. **70**, 437 (2001).
- 34) K. Kudo, Y. Koike, K. Maki, S. Tsuji, and K. Kumagai, J. Phys. Chem. Solids **62**, 361 (2001).
- 35) K. Naruse, T. Kawamata, M. Ohno, Y. Matsuoka, K. Kumagai, and Y. Koike, Solid State Commun. **154**, 60 (2013).
- 36) A. V. Sologubenko, E. Felder, K. Ginnó, H. Ott, A. Voekine, and A. Revcolevschi, Phys. Rev. B **62**, R6108 (2000).
- 37) A. V. Sologubenko, K. Ginnó, and H. R. Ott, Phys. Rev. B **64**, 054412 (2001).
- 38) N. Takahashi, T. Kawamata, T. Adachi, T. Noji, and Y. Koike, AIP Conf. Proc. **850**, 1265 (2006).
- 39) T. Kawamata, N. Takahashi, T. Adachi, T. Noji, K. Kudo, N. Kobayashi, and Y. Koike, J. Phys. Soc. Jpn. **77**, 034607 (2008).
- 40) T. Kawamata, N. Kaneko, M. Uesaka, M. Sato, and Y. Koike, J. Phys.: Conf. Ser. **200**, 022023 (2010).
- 41) N. Hlubek, P. Pibeiro, R. Saint-Martin, A. Revcolevschi, G. Roth, G. Behr, B. Büchner, and C. Hess, Phys. Rev. B **81**, 020405(R) (2010).
- 42) K. Momma and F. Izumi, J. Appl. Crystallogr. **44**, 1272 (2011).

Figure captions

Fig. 1. (color online) Crystal structure of CuB_2O_4 . (a) A $\text{Cu}_\text{A}\text{O}_4$ square (red) is connected with a $\text{Cu}_\text{B}\text{O}_4$ (blue) square through a BO_4 tetrahedron. (b) Only Cu_A (red) and Cu_B (blue) sites are drawn. Cu_A sites form a three-dimensional structure, while Cu_B sites form zigzag chains along the c -axis.

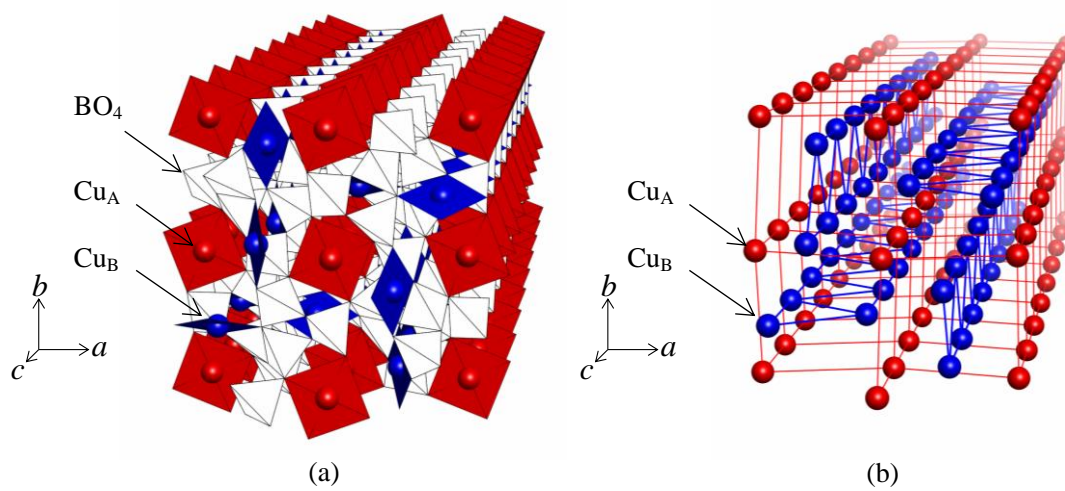


Fig. 2. (color online) Magnetic structures of CuB_2O_4 (a) in the commensurate weak ferromagnetic phase (C phase) of Cu_A^{2+} spins below T_N and (b) in the incommensurate helical phase (IC phase) of Cu_A^{2+} and Cu_B^{2+} spins below T^* .²⁰⁾ In (a), Cu_A^{2+} spins are almost pointing to the $[110]$ direction and $\sim 3^\circ$ canted within the ab -plane^{18,20)} and Cu_B^{2+} spins are nearly paramagnetic. Dashed lines indicate triangles formed with two adjacent Cu_A^{2+} spins and their nearest neighboring Cu_B^{2+} spin.

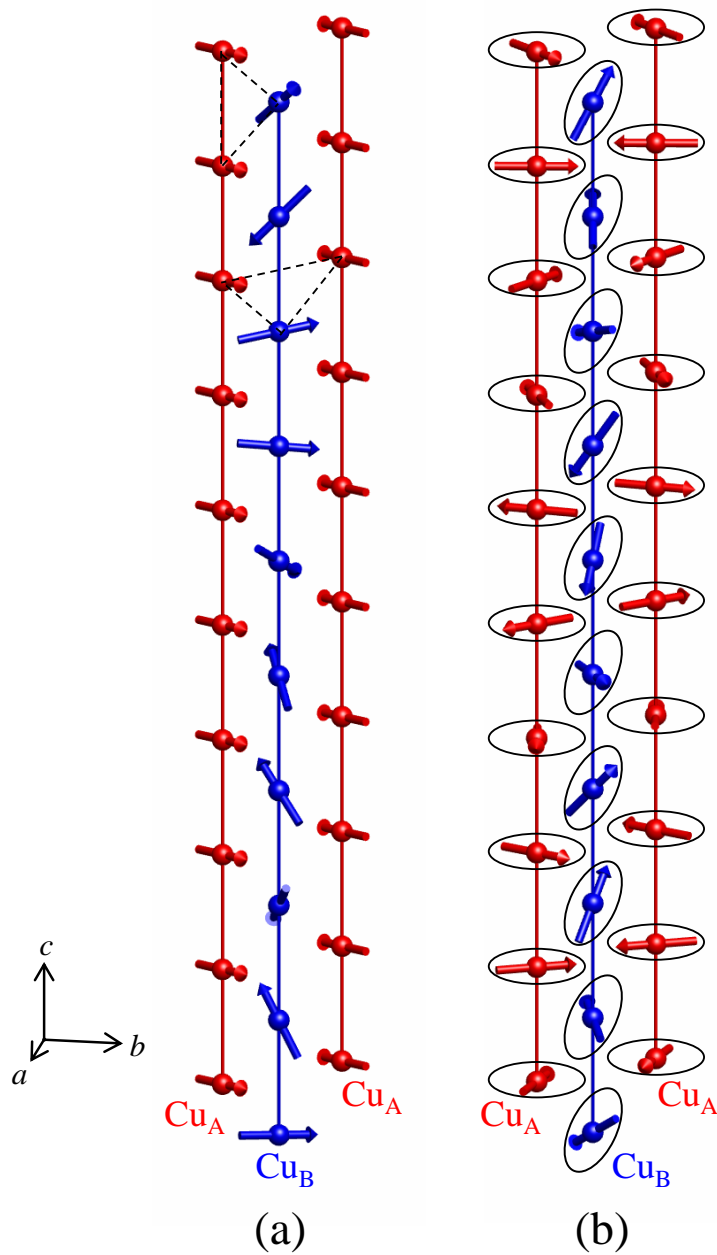


Fig. 3. (color online) Temperature dependences of the thermal conductivity along the c -axis, κ_c , and that along the $[110]$ direction, κ_{110} , in zero field for CuB_2O_4 . The inset shows enlarged plots of κ_c and κ_{110} at low temperatures. The data of κ_c in the inset are shifted upward by 100 W/Km.

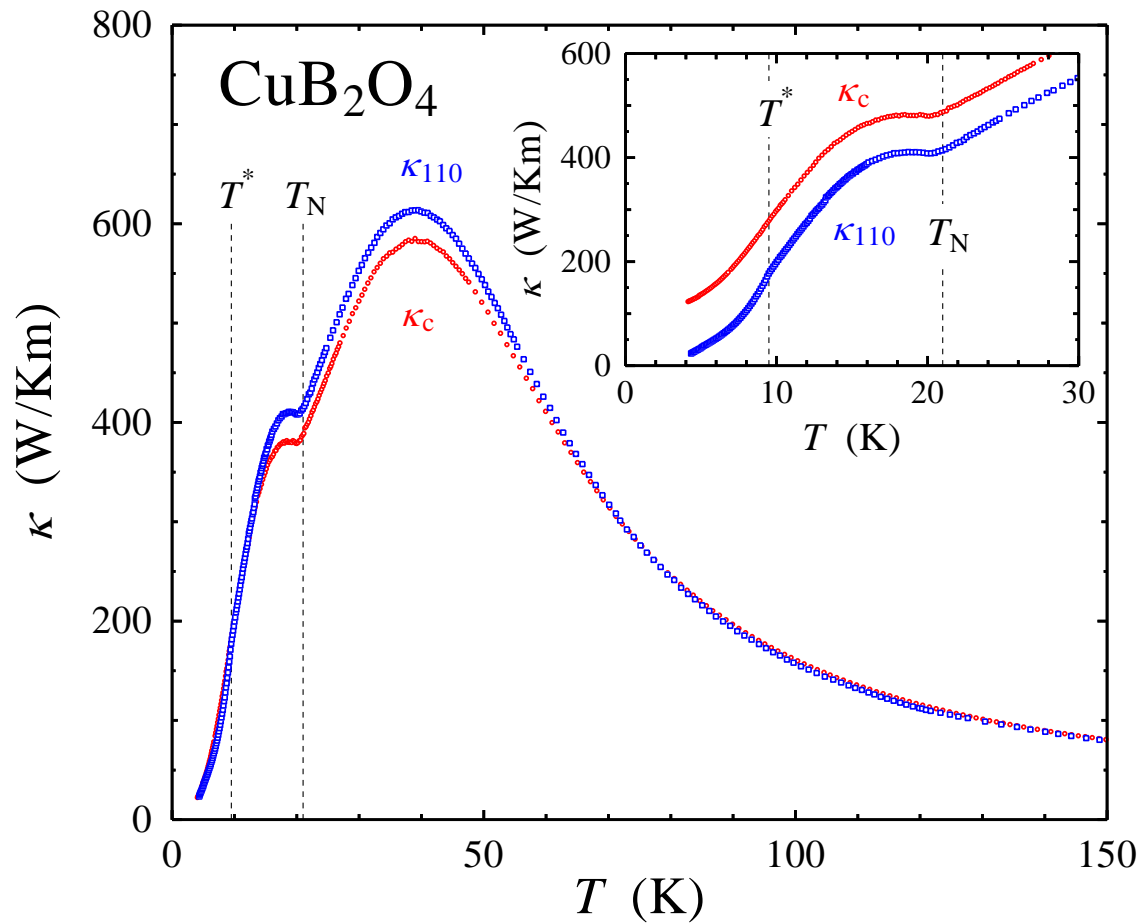


Fig. 4. (color online) Temperature dependences of the thermal conductivity along the [110] direction, κ_{110} , in magnetic fields (a) along the [110] direction and (b) along the c -axis for CuB_2O_4 . The data of κ_{110} in magnetic fields are shifted upward with increasing field 150 W/Km by 150 W/Km. Temperature dependences of κ_{110} divided by T^3 , κ_{110}/T^3 , in magnetic fields (c) along the [110] direction and (d) along the c -axis. The data of κ_{110}/T^3 in magnetic fields are shifted upward with increasing field 0.15 W/K⁴m by 0.15 W/K⁴m. Arrows indicate temperatures where κ_{110} or κ_{110}/T^3 changes markedly.

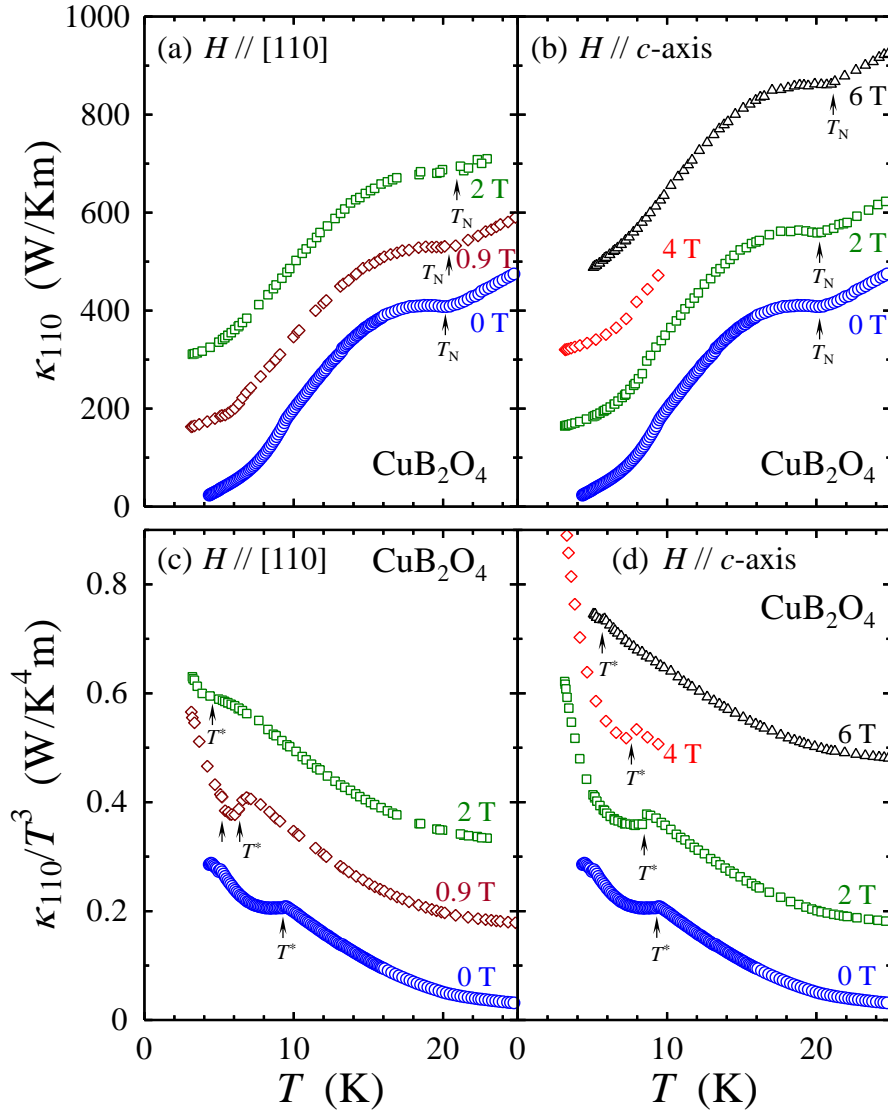


Fig. 5. (color online) Magnetic phase diagrams in magnetic fields (a) in the ab -plane and (b) along the c -axis for CuB_2O_4 . Closed and open circles indicate points shown by arrows in Figs. 4(a) - 4(d), and 6(a) - 6(b), where κ_{110} changes markedly, respectively. Solid lines indicate phase boundaries obtained by the ESR,^{14,19,27)} neutron scattering,²⁴⁾ nonlinear optical,²¹⁾ NMR,^{25,26)} μSR ,²²⁾ and magnetization²⁸⁾ measurements. The dashed line in (b) indicates the phase boundary due to the ferroelectric phase transition suggested by the ESR measurement.²³⁾

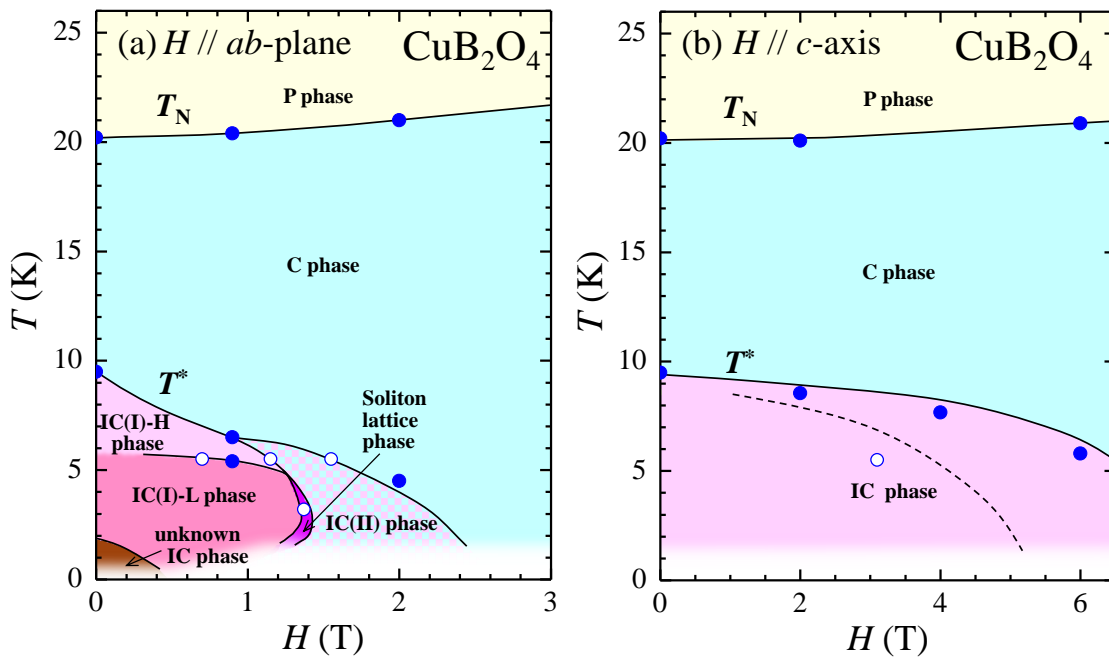


Fig. 6. Magnetic field dependences of the thermal conductivity along the [110] direction, κ_{110} , in magnetic fields (a) along the [110] direction and (b) along the c -axis at low temperatures of 3.2 K and 5.5 K for CuB_2O_4 . Arrows indicate magnetic fields where κ_{110} changes markedly.

